Separation and Purification Technology 274 (2021) 119034

Contents lists available at ScienceDirect

Separation and Purification Technology

journal homepage: www.elsevier.com/locate/seppur

Studies on the fouling behavior and cleaning method of pervaporation desalination membranes for reclamation of reverse osmosis concentrated water

Pengbo Zhao, Bowen Yao, Junquan Meng, Rui Zhang *, Bing Cao *, Pei Li *

College of Materials Science and Engineering, Beijing University of Chemical Technology, Beijing 100029, China

ARTICLE INFO

Keywords:
Pervaporation desalination
ROC reclamation
Membrane fouling
Membrane cleaning
COD

ABSTRACT

Pervaporation (PV), as a cost-efficient concentrating process, has been studied for Zero Liquid Discharge (ZLD) of desalination. Although high water flux and excellent salt rejection have been reported for many PV membranes. The desalination performance, fouling behavior, and cleaning protocol for treating real reverse osmosis concentrate (ROC) generated from industrial plants have never been studied. Meanwhile, understanding the fouling behavior and cleaning method in the treating process is crucial for the development of suitable PV desalination membranes. In this study, we used a lab-made PV membrane to treat industrial ROC with a high chemical oxygen demand (COD) value and high salt concentrations. The results showed that conductivity and COD of the produced water were below 20 μs/cm and 70 mg/L, respectively, which fulfilled the discharge standard. However, the membrane fouling problem was not trivial. To address the fouling issue, a chemical softening method was adopted to remove the calcium salts of the ROC, and a membrane cleaning method was developed to regenerate the water flux. As a result, a long-term water flux of 31.27 kg/m^2·h with a flux recovery rate of 98% were realized. This highlights the potential of PV desalination technology for ROC reclamation.

1. Introduction

As the demand for drinking water increases worldwide, the paradigm for selecting water sources is transitioning from fresh water resources to salt water and wastewater resources [1]. In order to produce water of superior quality, advanced desalination technologies have become more widespread to produce drinkable water seawater or wastewater sources [2]. Meanwhile, membrane-based desalination technology typically consumes less energy than conventional distillation method. Reverse osmosis (RO) is the most efficient desalination technology that occupies a 66% share of the global desalination capacity and produces nearly 21 billion gallons of water per day [3–5]. However, the reverse osmosis concentrated water (ROC), which accounts for about 20–25% of the produced water, has become a new source of pollution [6,7]. In general, ROC contains substantial amount of inorganic and organic foulants [8,9]. Chemical oxygen demand (COD) is one of the most commonly used pollution indicators in environmental discharge standards [10]. The high amount of COD makes ROC fail to meet the effluent discharge standards [11]. In order to reduce the ROC amount and meet the discharge standards, new ZLD technologies have been developed, which include membrane-based and thermal-based technologies or a combination of both [12,13]. For instance, compared to traditional distillation processes, membrane distillation (MD) operates at 60–80 °C and provides a large contact area per unit of equipment volume to achieve high productivity [14–16]. But the fouling problem of MD is a nightmare because of its hydrophobic surface. Nanofiltration (NF) is also a promising technology for treating ROC due to its high rejection to bivalent ions and organic compounds and low rejection to monovalent ions. These characters enable NF to remove most of COD, suspended solids and bivalent ions at much lower *trans*-membrane pressure than RO [17,18]. However, NF membrane is prone to pore plugging, which is more severe in the case of treating industrial ROCs [19]. Meanwhile, the operating pressure of NF is still high, that inevitably escalates fouling due to the concentration polarization.

Recently, pervaporation has been developed rapidly to treat concentrated salt solution, whose hydrophilic dense layer enable excellent fouling resistance [20]. Moreover, its hydrophilic dense layer solves the pore-wetting issue of MD membranes or pore plugging problem of NF membranes. In order to study the fouling behavior of PV desalination membranes, our group have used organic matters (HA, SA, Tween-20), inorganic salts (NaCl, $CaCl_2$) or a combination of them to

* Corresponding authors.
E-mail addresses: zhangrui1@mail.buct.edu.cn (R. Zhang), bcao@mail.buct.edu.cn (B. Cao), lipei@mail.buct.edu.cn (P. Li).

https://doi.org/10.1016/j.seppur.2021.119034
Received 15 April 2021; Received in revised form 24 May 2021; Accepted 24 May 2021
Available online 29 May 2021

Nomenclature

PV	Pervaporation
RO	Reverse osmosis
NF	Nanofiltration
ROC	Reverse osmosis concentrated water
ZLD	Zero Liquid Discharge
COD	chemical oxygen demand
MD	membrane distillation
HA	Humic acid
SA	Sodium alginate
CA	citric acid
SDS	sodium dodecyl sulfate
P(AA-AMPS)	poly (acrylic acid co-2-acrylamido-2-methyl propane sulfonic acid)
PVA	Polyvinyl alcohol
EOM	Effluent Organic Matter
FRR	flux recovery ratio
FDR	flux drop rate
VOC	volatile organic compounds

Table 1
The properties of the ROC before and after chemical softening.

Components	ROC	Softened ROC
Ca^{2+}(mg/L)	1298	23
K^{+}(mg/L)	224	220
Mg^{2+}(mg/L)	366	126
Na^{+}(mg/L)	24,550	33,306
Ba^{2+}(mg/L)	1.5	0.5
Zn^{2+}(mg/L)	4008	4000
Fe^{2+}(mg/L)	2.0	2.0
Cu^{2+}(mg/L)	1.6	1.6
NO_3^-(mg/L)	4.0	1.2
SO_4^{2-}(mg/L)	3026	3033
Cl^-(mg/L)	20,100	25,150
HCO_3^-(mg/L)	102	–
pH	6.64	6.64
Total nitrogen(mg/L)	20.5	20
Conductivity(ms/cm)	51.2	49.5
COD (mg/L)	860	840

mimic fouling environment [21–23]. However, the fouling behavior of PV desalination membranes to treat real wastewater has not been studied till now.

In this work, we aim to evaluate the potential of PV desalination membrane to produce water from ROCs and identify whether the quality of the produce water fulfills the discharge standard. The ROC is collected from the Inner Mongolia Tianhe Water Co., Ltd. that contains a high COD and high concentration of inorganic salts. We studied the fouling behavior and explored the suitable cleaning method of a PV desalination membrane for treating the ROC. To our best knowledge, this is the first study focusing on using PV technology to treat industrial ROC.

2. Materials and methods

2.1. Materials

Polyvinyl alcohol (PVA, Mw: 105,000 g·mol^{-1}), 30 wt% poly (acrylic acid co-2-acrylamido-2-methyl propane sulfonic acid) (P(AA-AMPS)) water solution, citric acid (CA) and sodium dodecyl sulfate (SDS, CP grade) were purchased from Sigma-Aldrich. Sodium carbonate (Na_2CO_3, purity: 99.8%) and sodium chloride (NaCl, AR grade) were obtained from Aladdin–Holdings Group (China). The reverse osmosis concentrate

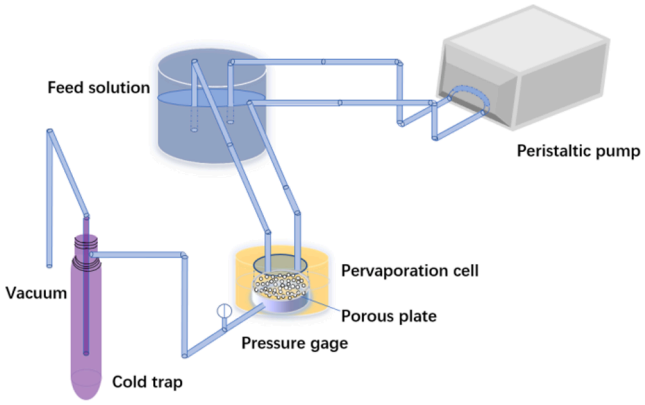

Fig. 1. A schematic diagram of the pervaporation device.

(ROC) was kindly provided by Inner Mongolia Tianhe Water Co., Ltd. The ion composition and other properties of ROC and softened ROC were listed in Table 1. pH and conductivity were determined using a pH meter (PHS-25, Shanghai Precision Scientific Instrument Co., Ltd, China) and a conductivity meter (DDSJ-308F, Thermo Fish OAKTON, Singapore). The chemical oxygen demand (COD) value was measured by a chemical oxygen demand tester (COD, CM-02, Shanghai Electronic Products Co., Ltd, China).

Since Ca^{2+} can form complexes with the constituents of Effluent Organic Matter (EOM), and aggregate membrane fouling [24,25], and it was removed from the ROC by chemical softening prior to PV desalination. Specifically, an excess amount of sodium carbonate was added to the ROC solution and stirred for 10 min. The solution was standing for several hours, and filtered. pH of the filtrate was adjusted to 6.64 using HCl or NaOH.

2.2. Fabrication of PV composite membranes

The P(AA-AMPS) crosslinked PVA/PVDF composite membranes were prepared using a spray-coating method introduced in our previous study [21]. First, a 3 wt% PVA water solution and a 30 wt% P(AA-AMPS) solution were mixed in a PVA/P(AA-AMPS) mass ratio of 7:3, and then the mixture was diluted to 1 wt% and sprayed onto a lab-made PVDF ultra-filtration membrane. The mean pore diameter and surface porosity of the PVDF membrane were 15 nm and 5.0%, respectively. At last, the PVA/PVDF composite membrane was thermally crosslinked at 100 °C for 30 min. The membrane surface was washed using DI water for 3 times before use.

2.3. Determination of the salt enrichment factors in the ROC

Table 1 showed that the ROC contained 12 anions and cations. We expected that the inorganic fouling would occur when their concentrations were over saturate. We defined a salt enrichment factor (Z), representing the lowest enrichment factor of the ROC to reach the saturate salt concentration. Z was calculated by Eqs. (1) and (2) [26]:

$$\omega = min\{\omega_A \times m | \omega_B \times n\} \tag{1}$$

$$Z = \frac{W_t}{W_a} = \frac{\frac{S}{S+100}}{\frac{\omega}{\rho} \times 10^{-6}} \tag{2}$$

where ω, ω_A and ω_B were the mass concentrations (mg/L) of salt ($A_m^{n+}B_n^{m-}$), cation (A^{n+}) and anion (B^{m-}), respectively. W_t and W_a were the theoretical maximum concentration and the initial concentration of salt, respectively. S was the solubility of salt (g/100 g) and ρ was the solution density (g/mL). Small Z meant that the salt was easier to precipitate from the feed solution and led to membrane fouling.

Table 2
Information of the cleaning methods.

Number	Cleaning Method	Number	Cleaning Method
A	ultrasonic vibration (30 min)	F	2% CA (15 min), then 0.1% NaOH (15 min)
B	2% CA (30 min)	G	0.1% NaOH (15 min), then 2% CA (15 min)
C	0.1% NaOH (30 min)	H	0.1% NaOH (15 min), then 0.02% NaClO (15 min)
D	0.01% SDS, pH = 12 (30 min)	I	0.1% NaOH (15 min), then ultrasonic vibration (15 min)
E	0.02%NaClO (30 min)	J	0.02%NaClO(15 min), then ultrasonic vibration (15 min)

2.4. Pervaporation desalination tests

Desalination properties were measured by a bespoke PV set-up shown in Fig. 1 [22]. The effective membrane area was 3.8 cm^2. The feed solutions comprising 3.5, 7.0, 10, 15, 17, 20 and 25 wt% NaCl were circulated on the membrane feed side at 65 °C. The permeate side of the membrane was 100 Pa. To study the effect of concentration polarization, membrane fluxes were recorded on feed flow rates at 0.5, 1.0, 1.5, 1.75 and 2.0 m/s, respectively using a 20 wt% NaCl solution as feed. At the membrane permeate side, water vapor was condensed in a liquid nitrogen cold trap every 10 min and weighted. An average mass of three independent experiments were used to calculated membrane flux using Eq. (3):

$$J_A = \frac{m}{s \times t} \tag{3}$$

where m was the mass of water vapor (kg); s was the effective membrane area (m^2); t was the testing time (h). While the theoretical flux (J_T) of the membrane was calculated by the following equation:

$$J_T = \overline{P_W} \times \Delta P \tag{4}$$

$$\overline{P_W} = \frac{J_A}{\Delta P} \tag{5}$$

where $\overline{P_W}$ was the water permeance, ΔP was the pressure difference across membrane, J_A was the water flux. The salt concentrations of feed and permeate solutions were measured by a conductivity meter. The permeate solution was used to wash the permeate side of the membrane to dissolve crystalized salt. Salt rejection (R) was determined using equation (6):

$$R = \left(\frac{C_f - C_p}{C_f}\right) \times 100\% \tag{6}$$

where C_f and C_p were the salt concentrations of the feed and permeate solutions.

To clarify the relation between water flux and vacuum pressure, water fluxes were determined at pressures of the membrane permeate side of 0.1, 2, 4, 6 and 10 kPa, respectively. Temperature of the water vapor at the permeate side was measured by a Thermocouple Temperature Meter (AS887, China). The dew point of the water vapor was calculated by the Anthony Eq. (7) [27]:

$$logP_W = A - B(T - C)^{-1} \tag{7}$$

where P_w was the partial pressure (Pa) and T was the temperature (°C) of the saturated vapor; A, B and C were empirical constants. Dew point of water vapor (T_d) between −45 and 60 °C was calculated by Eq. (8) [28]:

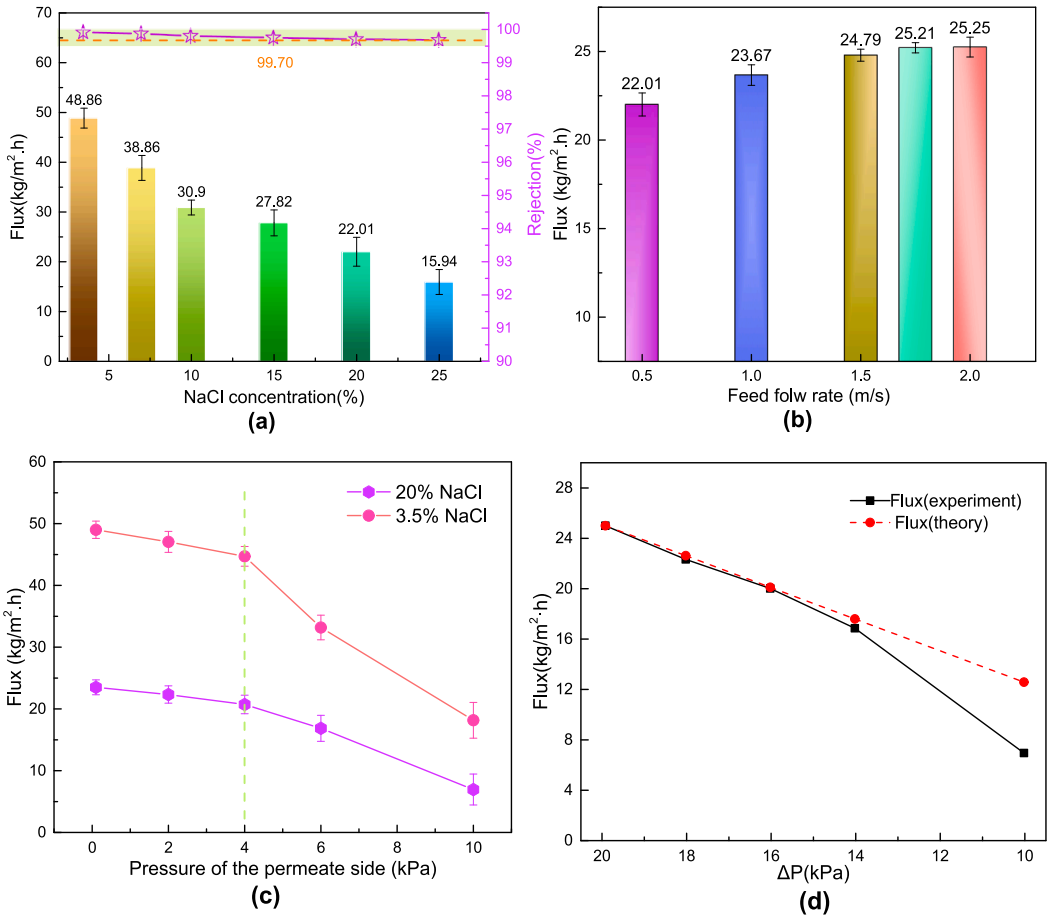

Fig. 2. (a) The water flux and rejection of the PV membranes using the feed solutions containing 3.5–25 wt% NaCl at 65 °C and a 0.5 m/s feed flow rate; (b) the changes in water flux with the feed flow rates using a 20 wt % NaCl solution as feed at 65 °C; (c) the changes in water fluxes with the permeate pressures at 65 °C and a 0.5 m/s feed flow rate; (d) the relationship between theoretical flux and experimental flux and pressure difference across membrane using a 20 wt% NaCl solution as feed at 65 °C.

$$T_d = \frac{243.12 ln \frac{P_W}{611.12}}{17.62 - ln \frac{P_W}{611.2}} \quad (8)$$

2.5. Membrane cleaning methods

The chemical cleaning agents included an acid cleaning agent (2 wt% citric acid (CA)), an alkaline cleaning agent (0.1 wt% NaOH solution), an anionic surfactant (0.01 wt% sodium dodecyl sulfate water solution (SDS)), and an oxidizing cleaning agent (0.02% NaClO water solution). The cleaning methods were numbered as listed in Table 2.

2.6. Fouling and cleaning experiments

The PV desalination experiments were carried out using the ROC as feed at 65 °C to study the membrane fouling behavior and optimize the cleaning method. In a specific experiment, a membrane flux was first measured in the initial 10 min, denoted as J_{W1}. The experiment was running for 6 h and the flux of the last 10 min was recorded as J_{W2}, representing the flux of the fouled membrane. After that, the fouled membrane was cleaned using cleaning method A. Then the cleaned membrane was used for PV desalination experiment again for 6 h, followed by cleaning using cleaning method B. The fouling experiment and membrane cleaning processes were repeated until all cleaning methods were attempted. Note that, the conductivity of the permeate solution was measured every 10 min to ensure the integrity of the membrane. The flux recovery ratio (*FRR*) and flux drop rate (*FDR*) were calculated using the following expressions:

$$FRR = \frac{J_{W2}}{J_{W1}} \times 100\% \quad (9)$$

$$FDR = \frac{J_{W1} - J_{W2}}{J_{W1}} \times 100\% \quad (10)$$

The permeate solution was collected every 20 min during a fouling test. The conductivity, COD, organic matters and total nitrogen of the permeate solution were determined. Note that, the organic matters in the ROC were mainly low boiling point, volatile organic chemicals, which were indicated by gas chromatography mass spectrometry (Trace ISQ China). While the total nitrogen (NH_3-N) was tested by a UV–Vis spectrophotometry (Thermo Evolution 201 USA) [29].

2.7. Membrane characterization

A scanning electron microscope (SEM) (HITACHI S-7800 Japan) was used to determine surface morphologies of the virgin PV membranes, fouled membranes and chemical cleaned membranes. The chemical elements of the fouled membranes' surfaces were analyzed by EDS (FEI Nova Nano SEM and Hitachi S3400 USA) and XPS (ESCALAB 250 Japan).

3. Results and discussion

3.1. Desalination property of the PV composite membrane

The effect of salt concentration, feed flow rate, and permeate pressure on desalination properties of the PV composite membrane at 65 °C were given in Fig. 2. The water fluxes of PV membrane decreased from 48.9 ± 1.5 kg/m^2·h to 15.9 ± 2.9 kg/m^2·h as the salt concentrations increased from 3.5 to 25 wt%. This was caused by the reduced water driving force at higher salt concentrations and concentration or temperature polarization effects of the salt solution near the membrane surface [30]. The high salt rejections over 99.70% demonstrated the excellent salt rejection property of the PV membranes for treating concentrated brine solutions. It has been reported that when the feed solution was on a turbulent state ($Re > 2000$), the concentration/temperature polarization effect would be greatly mitigated [31]. As shown in Fig. 2b, the water fluxes of PV membranes increased with the increment in the flow rates of NaCl solutions. When the feed flow rates were 1.75 m/s and 2 m/s, the water fluxes became stable at 23.2 ± 0.1 kg/m^2·h, indicating that the concentration polarization effect had been reduced to a low level [32]. Note that, the *Re* number was 4200 at a flow rate of 0.5 m/s. Hence all the feed solutions were controlled at turbulent flow conditions. Fig. 2c shown that the water flux decreased as the pressure of permeate side increasing. The increment in the membrane permeate pressure caused the vapor pressure gradient (ΔP) across the membrane to decrease. Moreover, as the permeate pressure was higher than 4 kPa, the water flux decreased more rapidly. In Fig. 2d, the theoretical flux was close to the experimental flux under the high pressure difference across membrane (ΔP), while the experimental flux was obviously lower than theoretical flux under low pressure difference across membrane. This was because the water vapor cannot be completely condensed in the cold trap at such high pressure. As listed in Table 3, when the permeate side pressure was greater than 4 kPa, the temperature of water vapor was very close to its dew point. Therefore, part of the water vapor was condensed on the walls and pipes at the membrane permeate side.

Table 3
Dew point and permeate side temperature at different permeate side pressures.

Permeate pressure (kPa)	Dew point (°C)	T of the permeate side (°C)
0.1	−20.33	34.8 ± 4
2	15.19	34.3 ± 4
4	24.88	34.1 ± 3
6	30.86	34.2 ± 3
10	38.75	33.8 ± 3

Table 4
The enrichment factors to induce precipitation of salts in the ROC.

Enrichment factor	Cl^-	SO_4^{2-}	HCO_3	NO_3^-
K^+	987.5	410.93	3172.7	4143.6
Na^+	**21.89**	100.3	2795.8	643.07
Ca^{2+}	1977.1	**5.2**	–	201.7
Mg^{2+}	287.9	478.7	–	163
Ba^{2+}	63,348	**9.89**	–	–
Zn^{2+}	19,878	755,215	–	–
Fe^{2+}	108,515	–	–	–
Cu^{2+}	187,070	524,725	–	–

Table 5
The enrichment factors to induce precipitation of salts in the softened ROC.

Enrichment factor	Cl^-	SO_4^{2-}	NO_3^-
K^+	790	408.8	4144
Na^+	**17.52**	31.73	472.9
Ca^{2+}	216.9	**156.9**	6050
Mg^{2+}	4580	1435	490
Ba^{2+}	167,238	**33**	–
Zn^{2+}	15,902	752,950	–
Fe^{2+}	86,812	–	–
Cu^{2+}	149,656	186,500	–

3.2. The enrichment factors of the ROC

The enrichment factors to cause salt precipitations of the ROC and the softened ROC were listed in Table 4 and Table 5, respectively. Since $CaSO_4$ and $BaSO_4$ had the lowest enrichment factors in the ROC, the two salts were most likely to precipitate in a PV desalination process. NaCl had the third lowest enrichment factor of 21.89. Hence, NaCl may also scale on membrane surface due to concentration polarization. Other salts were difficult to precipitate because their enrichment factors were much higher. This was caused by either the low initial concentration or

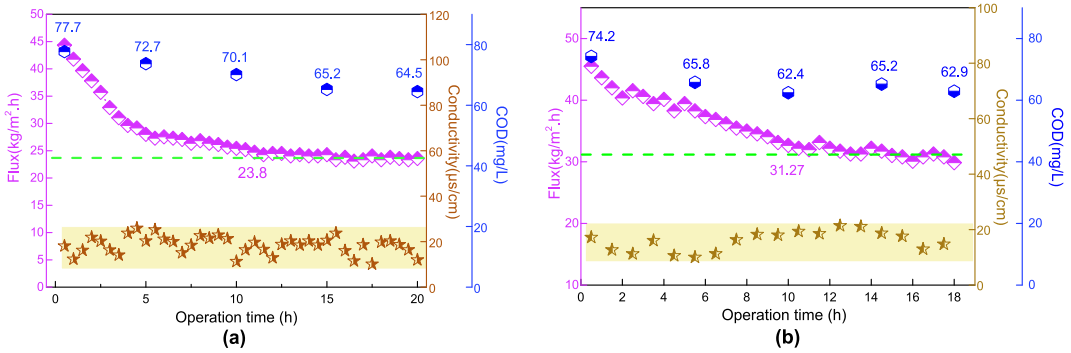

Fig. 3. The 20 h water flux, conductivity and COD of the PV membrane using (a) the ROC and (b) the softened ROC as feed solutions at 65 °C with a 1.75 m/s feed flow rate.

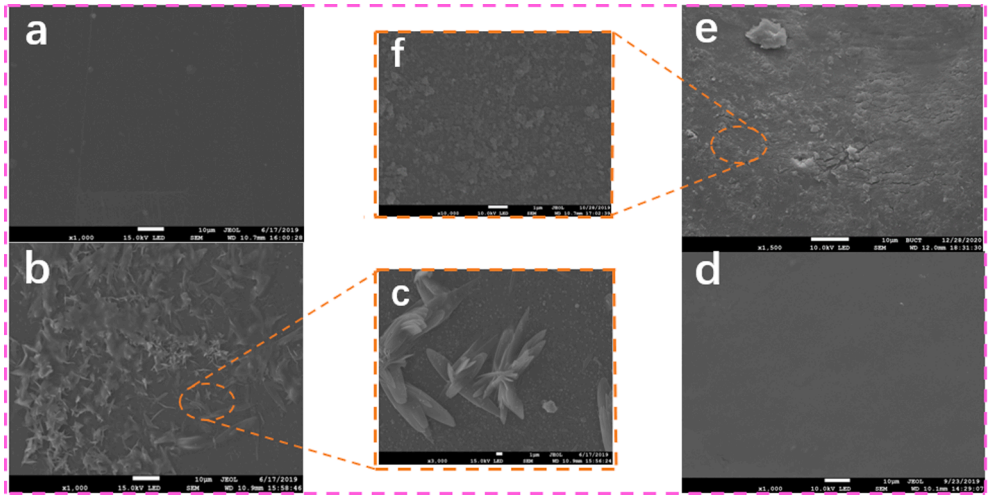

Fig. 4. SEM images of the surface morphologies of the pristine PV membranes (a, d); the membranes (b, c) fouled by ROC for 20 h; and the membranes (e, f) fouled by the softened ROC for 18 h.

high saturate concentration of the salts. To alleviate the scaling tendency, a chemical softening treatment was carried out to lower the concentrations of Ca^{2+} and Ba^{2+} in the ROC. As listed in Table 1, the concentrations of Ca^{2+} and Ba^{2+} reduced by 98% and 70%, respectively, and the enrichment factors to $CaSO_4$ and $BaSO_4$ increased to 156.9 and 33, much higher than the enrichment factor of NaCl (17.52). Hence, NaCl was the most likely salt to cause inorganic fouling in the softened ROC solution. Since the lowest enrichment factor (17.52) of the softened ROC was 3 times higher than that of the untreated ROC, the fouling phenomenon shall be greatly inhibited. To further control the

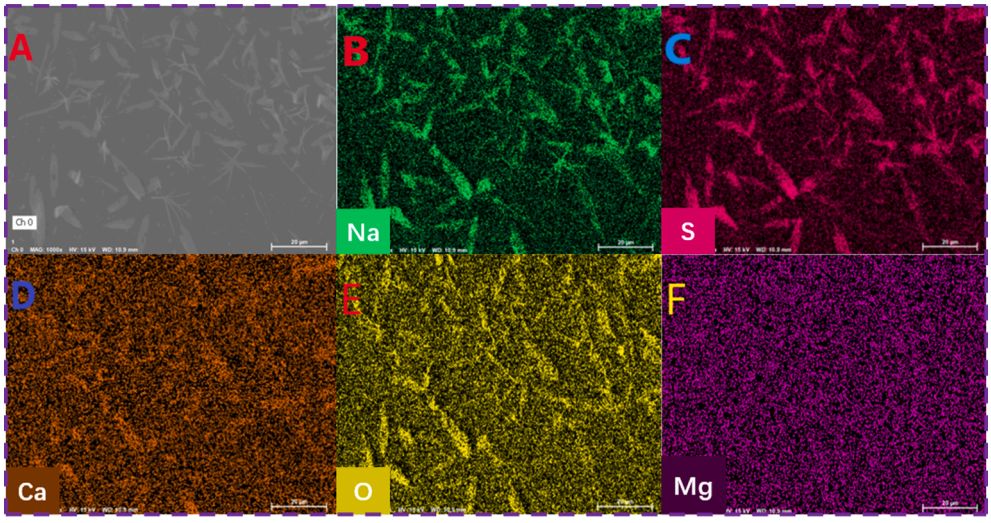

Fig. 5. (a) The SEM image of the membrane surface fouled by ROC; EDS of sodium (b), sulfur (c), calcium (d), oxygen (e) and magnesium (f) of the fouled membrane surface.

Table 6
Contaminant composition on membrane surface fouled by ROC and softened ROC.

Element	Element content of pristine membrane (%)	Element content of membrane fouled by ROC (%)	Element content of membrane fouled by softened ROC (%)
C	46.77	5.98	55.95
O	50.27	50.56	41.59
Na	2.59	1.96	1.78
Mg	0.11	0.29	0.13
S	0.26	16.44	0.42
Ca	0	21.72	0
Cl	0	2.00	0
Ba	0	0.95	0
F	0	0.80	0.12
Total	100	100	100

membrane fouling, the feed flow rate was increased to 1.75 m/s to mitigate the concentration polarization effect.

3.3. Membrane fouling and characteristics

The water fluxes, permeate conductivity and COD of the PV membranes were shown in Fig. 3 using the ROC and softened ROC as feeds with a flow rate of 1.75 m/s at 65 °C. As shown in Fig. 3a, the water fluxes decreased from 45 kg/(m^2·h) to 23.8 kg/(m^2·h) in the first 10 h and then became stable in the rest 10 h. As shown in Fig. 4b and c, salt crystals appeared on the membrane surfaces. On one hand, carboxyl groups in organic matters intended to interact with Ca^{2+} and form organic fouling on membrane surface [33]. On the other hand, the Ca^{2+} concentration near the membrane surface would be higher than in the bulk solution so that facilitated the formation of $CaSO_4$ crystal. Therefore, the fouling problem was very serious when the untreated ROC was used as feed.

The surface elemental compositions of the pristine and fouled PV membrane were analyzed by EDS as shown in Fig. 5 and Table 6. Fig. 5 showed that the petal-like crystals consist of Ca, S, O and a small amount of Na. Hence, the petal-like crystals were $CaSO_4$. Table 6 listed the element contents on the surfaces of clean and fouled membranes. The contents of S, Ca, Cl, Ba, and F were higher in the fouled membrane compared to pristine membrane. It was another evidence of the formation of inorganic fouling on the membrane surface.

Fig. 3a showed that the conductivity of the permeate water was in a range of 10–25 μs/cm that indicated a salt rejection of 99.90%. The average COD of the permeate water was in a range of 64.5–77.7 mg/L that corresponded to a COD rejection over 90%. Although the COD rejection was lower than the salt rejection, a COD value of 70 ± 10 mg/L in the permeate water still fulfilled the discharge standard of 100 mg/L [34]. The relatively low COD rejection was caused by the poor rejection of the PV membrane to volatile organic compounds (VOCs).

Fig. 3b showed the 18 h PV desalination performance to the softened ROC. The water flux dropped by 30%, less than the 47% flux reduction when using ROC as feed. The conductivities of the permeate water were within 20 μs/cm that corresponded to salt rejection over 99.95%. While the COD varied between 62.9 and 74.2 mg/L that corresponded to a COD rejection over 91%. Hence, the salt and COD rejection of the PV membrane to the softened ROC were similar as the untreated ROC. However, the higher membrane flux demonstrated that the water softening treatment could effectively improve the desalination property.

The SEM images of the fouled membrane surface after the long-term fouling test were shown in Fig. 4e and f. A cake layer was formed on the membrane surface without observable salt crystals. This was mainly because most of the Ca^{2+} and Ba^{2+} had been removed by the water softening treatment. The peak intensity at 3000 cm^{-1} representing C—H was stronger than the pristine membrane (Fig. 6a), indicating that the membrane surface was fouled by organic matters. As shown in Fig. 6b, the fouled membrane had a new peak at 695 eV (representing F1s), indicating that the organic fouling contained fluorine. This demonstrated that hydrophobic organics tend to foul the hydrophilic membranes. Table 7 listed the types and concentrations of VOC in the softened ROC and permeate water. Obviously, the organics with small molecular weights existed in the permeate water. Moreover, the COD concentration in the permeate water decreased with the operating time. This might be due to that the cake layer formed on the membrane surface limited the transfer of organics. Meanwhile, the total nitrogen (NH_3-N) concentrations of the permeate water were 20 ± 1.5 and 18.5 ± 1.2 mg/L, respectively, for the ROC and softened ROC feed solutions. This meant that the PV membrane had a limited rejection to ammonia. The presence of a small amount of total nitrogen should be the reason of the relatively high conductivity (20 μs/cm) of the permeate water.

Table 7
The organic compounds in the softened ROC and the permeate water.

Organic matters	Content of the softened ROC (%)	Content of the produced water (%)
C_2Cl_4	1.5	13.2
C_2Cl_6	2.1	18.3
$C_{26}H_{54}$	0.2	2.5
$C_{12}H_{11}N$	0.7	6.4
$C_{16}H_{22}O_4$	1.4	12.4
$C_{16}H_{18}N_2O_2S$	5.6	52.8
$C_{14}H_{22}O$	17.7	–
$C_{18}H_{35}BrO_2$	12.6	–
$C_{20}H_{40}O_2$	25.9	–
$C_{16}H_{16}Cl_3N_3$	32.3	–

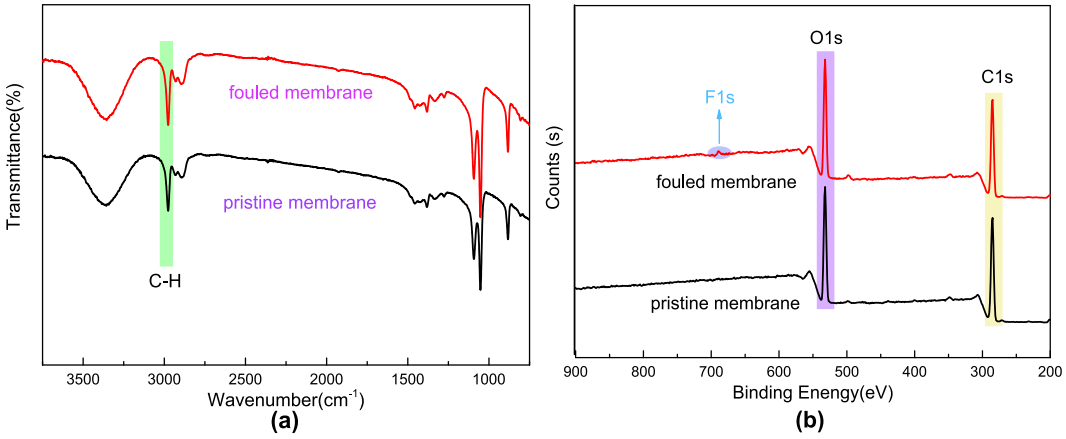

Fig. 6. The FTIR spectra (a) and XPS (b) of the pristine membrane and the membrane fouled by the softened ROC.

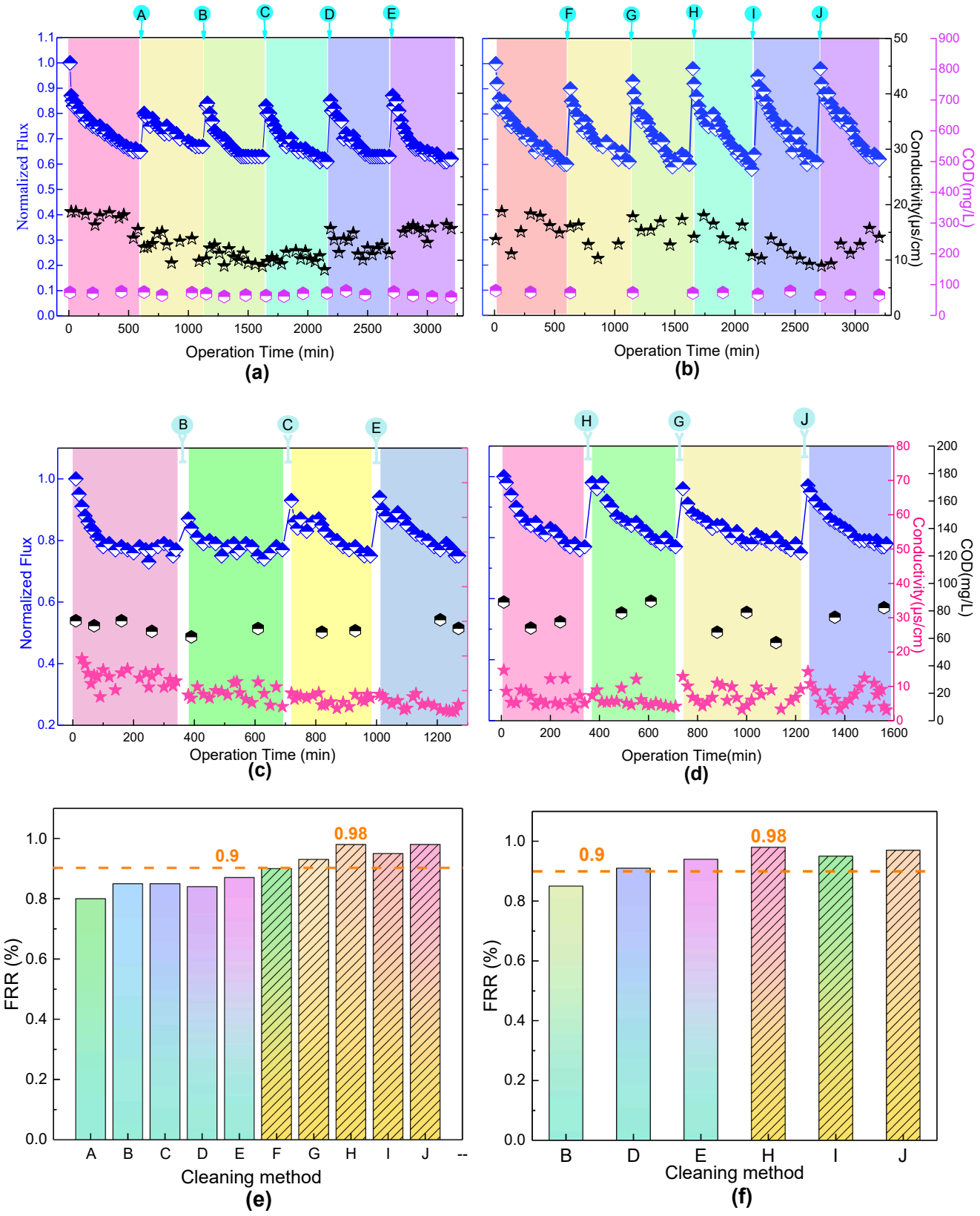

Fig. 7. (a, b) The long-term water flux, conductivity and COD using the ROC solution as feed using cleaning methods of A to J; (c, d) the long-term water flux, conductivity and COD using the softened ROC as feed solution with cleaning methods of B, C, E, H, G, J; (e) the FRR of fouled membranes by cleaning methods of A to J when using ROC as feed solution; (f) the FRR of fouled membranes using cleaning methods of B, C, E, H, G, J when using softened ROC as feed solution.

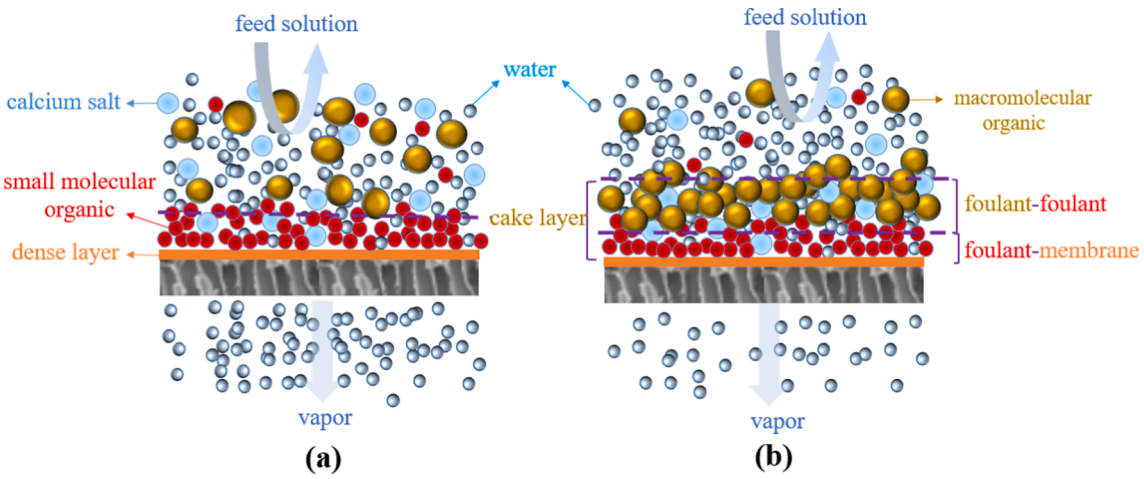

Fig. 8. Schematic diagram of two stages of membrane fouling.

3.4. *Cleaning of the fouled membranes*

Ten methods (listed in Table 2) were used to clean the fouled membranes to screen out the best cleaning method. As shown in Fig. 7a and b, the flux gradually decreased first and then became stable. Hence, the membrane fouling was divided into two stages. First, the foulants deposited or adsorbed on the membrane surface rapidly and the flux markedly reduced. After that, the flux became stable, which meant that an equilibrium between foulants accumulating and diffusing back to the bulk solution had been reached. Meanwhile, in the first stage, the foulants were mainly small molecular weight organics, and in the second stage, macromolecular weight organic matters and inorganic salts deposited on membrane surface and formed a cake layer (Fig. 8) [35]. Based on the types of interactions between the membrane surface and foulants, the membrane fouling could be classified into foulant-membrane interaction and foulant-deposited foulant interaction [36,37]. Typically, the rate and extent of organic fouling were determined by the foulant-foulant interactions because the monolayer coverage on the membrane surface through foulant-membrane interactions was attained in a very short period [38].

After the 10 h fouling test, the fouled membrane was cleaned using method A to E. For method A, membrane was ultrasonic cleaned for 30 min, and the flux recovery was up to 80%. Hence physical cleaning could only remove part of the unstable foulants. For method B, citric acid was adopted since it could dissolve $CaCO_3$ of the cake layer to loosen the cake layer and make it easier to be washed off. For method C, NaOH was used because it decomposed organic fouling. For method D, SDS as a surfactant was widely used to remove foulants through hydrophobic interactions [39]. SDS also decreased the surface tension at the fouling layer surface, thereby increasing the contact between the cleaning solution and foulants [40]. For method E, ClO^- could oxidize organics into small molecules. As shown in Fig. 7e, the FRR of method B, C and D were similar but higher than method A. This proved that chemical cleaning was better than physical cleaning. The highest FRR was obtained for method E, which meant that NaClO cleaning was the most effective method. However, all the FRR values were lower than 90% that meant the sole cleaning agent was not sufficient for fully recovery membrane flux. This was reasonable since alkali cannot disrupt the complexes formed by the organic foulants with multivalent cations like calcium ion [1]. Therefore, the fouled membranes were cleaning by combinations of methods from A to E. As shown in Fig. 7e, the highest FRR of 98% was achieved for method H where the membrane was washed by 0.1% NaOH solution for 15 min followed by 0.02% NaClO solution for 15 min.

As shown in Fig. 7 c and d, when using the softened ROC solution as feed, the flux dropped by 25%, much lower than the 40% drop in flux when using the ROC as feed. This result matched the data shown in

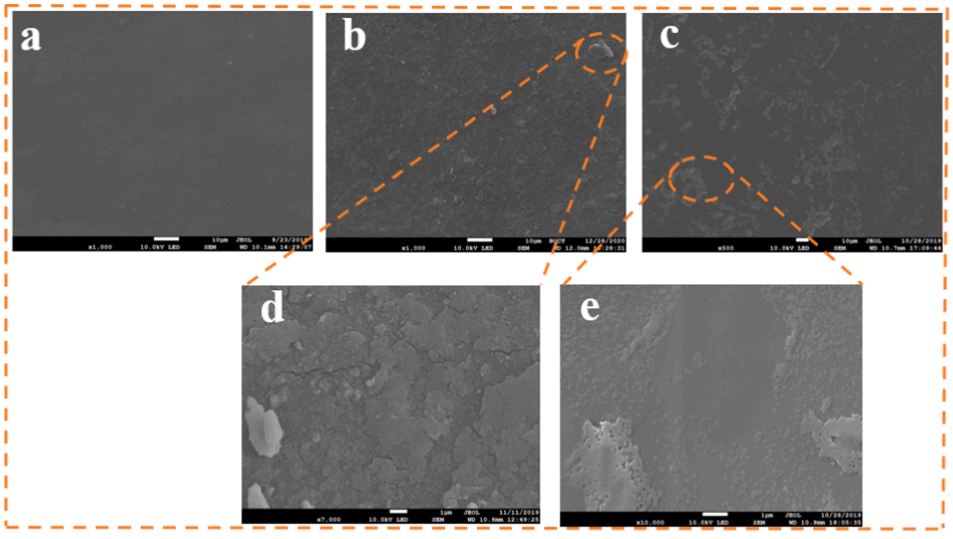

Fig. 9. The surface SEM images of (a) the pristine PV membranes; (b) and (d) the fouled membranes by the softened ROC; (c) and (e) the membranes cleaned using method H.

Fig. 3. It again proved that fouling of the ROC could be mitigated by the chemical softening treatment. Note that, no significant differences in the conductivity and COD values of the permeate solutions were observed when using ROC or softened ROC solutions as feed. This was reasonable since the conductivity and COD of the ROC solution before and after the chemical softening treatment were barely changed as listed in Table 1.

The surface images of the PV membrane during the fouling and cleaning experiments were obtained using SEM. As shown in Fig. 9a, surface of the PV membrane was very clean. After the fouling experiment, fouling compounds appeared on the membrane surface as shown in Fig. 9b and d. After cleaning using method H, most of the fouling materials have been removed but a small amount of foulants left on the surface as shown in Fig. 9c and e. This explained why the FRR was 98% not 100%.

4. Conclusion

A PVA-P(AA-AMPS)/PVDF composite membrane is prepared and used to extract water from ROC. The quality of produced water meets the discharge standard and the salt and COD rejection are 99.90% and 90%, respectively. The calcium ions of ROC aggravate the fouling problem. It is removed from the ROC by chemical softening and alleviates the fouling issue. The water flux can be best recovered to 98% by washing the fouled membrane using a combined cleaning process where the membrane is first washed by a 0.1% NaOH for 15 min, then a 0.02% NaClO solution for 15 min. This study provides valuable reference for recycling highly concentrated brine by PV technology.

Declaration of Competing Interest

The authors declare that they have no known competing financial interests or personal relationships that could have appeared to influence the work reported in this paper.

Acknowledgement

This research is funded by National Natural Science Foundation of China (51773011).

References

[1] W.S. Ang, A. Tiraferri, K.L. Chen, M. Elimelech, Fouling and cleaning of RO membranes fouled by mixtures of organic foulants simulating wastewater effluent, J. Membr. Sci. 376 (2011) 196–206.
[2] K.H. Mistry, R.K. McGovern, G.P. Thiel, E.K. Summers, S.M. Zubair, J.H. Lienhard V, Entropy generation analysis of desalination technologies, Entropy 13(10) (2011) 1829–1864.
[3] G.P. Thiel, E.W. Tow, L.D. Banchik, H.W. Chung, J.H. Lienhard V, Energy consumption in desalinating produced water from shale oil and gas extraction, Desalination 366 (2015) 94–112.
[4] S.G.J. Heijman, E. Rabinovitch, F. Bos, N. Olthof, J.C.V. Dijk, Sustainable seawater desalination: Stand-alone small-scale windmill and reverse osmosis system, Desalination 248 (1–3) (2009) 114–117.
[5] U. Caldera, U. Breyer, Learning curve for seawater reverse osmosis desalination plants: capital cost trend of the past, present and future, Water Resour. Res. 53 (12) (2017) 10523–10538.
[6] A.Y. Bagastyo, J. Keller, Y. Poussade, D.J. Batstone, Characterisation and removal of recalcitrants in reverse osmosis concentrates from water reclamation plants, Water Res. 45 (2011) 2415–2427.
[7] M. Umar, F. Roddick, L. Fan, O. Autin, B. Jefferson, Treatment of municipal wastewater reverse osmosis concentrate using UVC-LED/H_2O_2 with and without coagulation pre-treatment, Chem. Eng. J. 260 (2015) 649–656.
[8] S. Shanmuganathan, M.A. Johir, T.V. Nguyen, J. Kandasamy, S. Vigneswaran, Experimental evaluation of microfiltration–granular activated carbon (MF–GAC)/nanofilter hybrid system in high quality water reuse, J. Membr. Sci. 476 (2015) 1–9.
[9] S. Pradhan, L. Fan, F.A. Roddick, E. Shahsavari, A.S. Ball, Impact of salinity on organic matter and nitrogen removal from a municipal wastewater RO concentrate using biologically activated carbon coupled with UV/H_2O_2, Water Res. 94 (2016) 103–110.
[10] N. Kayaalp, M.E. Ersahin, H. Ozgun, I. Koyuncu, C. Kinaci, A new approach for chemical oxygen demand (COD) measurement at high salinity and low organic matter samples, Environ. Sci. Pollut. Res. 17 (2010) 1547–1552.
[11] E. Li, X. Jin, S. Lu, Microbial communities in biological denitrification system using methanol as carbon source for treatment of reverse osmosis concentrate from coking wastewater, J. Water Reuse nd Desalination 8 (3) (2018) 360–371.
[12] A. Subramani, J.G. Jacangelo, Treatment technologies for reverse osmosis concentrate volume minimization: A review, Sep. Purif. Technol. 122 (2014) 472–489.
[13] W.L. Song, L.Y. Lee, E.Y. Liu, X.Q. Shi, S.L. Ong, H.Y. Ng, Spatial variation of fouling behavior in high recovery nanofiltration for industrial reverse osmosis brine treatment towards zero liquid discharge, J. Membr. Sci. 609 (2020), 118185.
[14] C.R. Martinetti, A.E. Childress, T.Y. Cath, High recovery of concentrated RO brines using forward osmosis and membrane distillation, J. Membr. Sci. 331 (2009) 31–39.
[15] J. Mericq, S. Laborie, C. Cabassud, Vacuum membrane distillation of seawater reverse osmosis brines, Water Res. 44 (2010) 5260–5273.
[16] G. Naidu, S. Jeong, Y. Choi, S. Vigneswaran, Membrane distillation for wastewater reverse osmosis concentrate treatment with water reuse potential, J. Membr. Sci. 524 (2017) 565–575.
[17] M. Reig, S. Casas, O. Gibert, C. Valderrama, J.L. Cortina, Integration of nanofiltration and bipolar electrodialysis for valorization of seawater desalination brines: production of drinking and waste water treatment chemicals, Desalination 382 (2016) 13–20.
[18] J.W Zhai, J.T. Szczepanski, R.H. Xiong, Method for treating high concentration wastewater SUCH as RO brine, World Intellect. Prop. Organ. (WO 2014/089796 Al) (2014).
[19] A. Azaïs, J. Mendret, S. Gassara, E. Petit, A. Deratani, S. Brosillon, Nanofiltration for wastewater reuse: counteractive effects of fouling and matrice on the rejection of pharmaceutical active compounds, Separ. Purif. Technol. 133 (2014) 313–327.
[20] X.B. Yang, L.L. Yan, Y.D. Wu, Y.Y. Liu, L. Shao, Biomimetic hydrophilization engineering on membrane surface for highly-efficient water purification, J. Membr. Sci. 589 (2019), 117223.
[21] Y.L. Xue, J. Huang, C.H. Lau, B. Cao, P. Li, Tailoring the molecular structure of crosslinked polymers for pervaporation desalination, Nat. Commun. 11 (1) (2020).
[22] P.B. Zhao, Y.L. Xue, R. Zhang, B. Cao, P. Li, Fabrication of pervaporation desalination membranes with excellent chemical resistance for chemical washing, J. Membr. Sci. 118367 (2020).
[23] J.Q. Meng, P. Li, B. Cao, High-flux direct-contact pervaporation membranes for desalination, ACS Appl. Mater. Interfaces 11 (2019) 28461–32846.
[24] C. Jarusutthirak, G. Amy, J. Croue, Fouling characteristics of wastewater effluent organic matter (EfOM) isolates on NF and UF membranes, Desalination 145 (2002) 247–255.
[25] C. Ding, X. Zhang, S. Xiong, L. Shen, B.Y. Liu, Y. Wang, Organophosphonate draw solution for produced water treatment with effectively mitigated membrane fouling via forward osmosis, J. Membr. Sci. 593 (2020), 117429.
[26] B. Bolto, M. Hoang, T. Tran, Review of piezodialysis-salt removal with charge mosaic membranes, Desalination 254 (1–3) (2010) 1–5.
[27] L.A. Wood, The use of dewpoint temperature in humidity calculation, J. Res. Natl. Bureau Standards Section C Eng. Instrum. 74C (3–4) (1970) 117.
[28] R.R. Dreisbach. Physical Properties of Chemical Compounds, Vol. III, p. 474, Advances in Chemistry Series No. 29, American Chemical Society, Washington, 1961.
[29] L.B. Zheng, Y. D, G Wang, Z.G. Yue, C. Zhang, Y.W. Wang, J.Y. Zhang, J. Wang, G. L. Liang, Y.S. Wei, Characteristics and formation mechanism of membrane fouling in a full-scale RO wastewater reclamation process: Membrane autopsy and fouling characterization, J. Membr. Sci. 563 (2018) 843–856.
[30] B. Liang, W. Zhan, G. Qi, S. Lin, Q. Nan, Y. Liu, B. Cao, K. Pan, High Performance Graphene Oxide/Polyacrylonitrile Composite Pervaporation Membranes for Desalination Applications, J. Mater. Chem. A 3 (9) (2015) 5140–5147.
[31] Y.L. Xue, C.H. Lau, B. Cao, P. Li, Elucidating the impact of polymer crosslinking and fixed carrier on enhanced water transport during desalination using pervaporation membranes, J. Membr. Sci. 575 (2019) 135–146.
[32] Z. Xie, D. Ng, M. Hoang, T. Duong, S. Gray, Separation of aqueous salt solution by pervaporation through hybrid organic-inorganic membrane: effect of operating conditions, Desalination 273 (1) (2011) 220–225.
[33] S. Lee, W.S. Ang, M. Elimelech, Fouling of reverse osmosis membranes by hydrophilic organic matter: Implications for water reuse, Desalination 187 (2006) 313–321.
[34] J. Yang, H.X. Guo, B.B. Liu, R. Shi, B. Zhang, W.L. Ye, Environmental regulation and the pollution haven hypothesis: do environmental regulation measures matter? J. Cleaner Prod. 202 (2018) 993–1000.
[35] E.K. Lee, V. Chen, A.G. Fane, Natural organic matter (NOM) fouling in low pressure membrane filtration - effect of membranes and operation modes, Desalination 218 (2008) 257–270.
[36] J. Luo, W. Cao, L.H. Ding, Z.Z. Zhu, Y.H. Wan, M.Y. Jaffrin, Treatment of dairy effluent by shear-enhanced membrane filtration: the role of foulants, Sep. Purif. Technol. 96 (2012) 194–203.
[37] W.X. Zhang, W.Z. Liang, G.H. Huang, J. Wei, L.H. Ding, M.Y. Jaffrin, Studies of membrane fouling mechanisms involved in the micellar-enhanced ultrafiltration using blocking models, RSC Adv. 5 (60) (2015) 48484–48491.
[38] Q. Li, M. Elimelech, Organic fouling and chemical cleaning of nanofiltration membranes: measurements and mechanisms, Environ. Sci. Technol. 38 (2004) 4683.
[39] S.S. Madaeni, S. Samieirad, Chemical cleaning of reverse osmosis membrane fouled by wastewater, Desalination 257 (1–3) (2010) 80–86.
[40] L. Masse, J. Puig-Bargués, M. Mondor, L. Deschênes, Efficiency of EDTA, SDS, and NaOH solutions to clean RO membranes processing swine wastewater, Sep. Sci. Technol. 50 (2015) 16.